NOCA versus IDMA using UFMC for 5G Multiple Access

Mohammadhossein Attar*†, Yejian Chen†, Sher Ali Cheema*, Thorsten Wild†, and Martin Haardt*
*Communications Reserach Laboratory, Ilmenau University of Technology, D-98684 Ilmenau, Germany
Email: {mohammadhossein.attar, sher-ali.cheema, martin.haardt}@tu-ilmenau.de
†Nokia Bell Labs, Lorenzstrasse 10, 70435 Stuttgart, Germany
Email: {mohammadhossein.attar, yejian.chen, thorsten.wild}@nokia.com

***Abstract*—Non-orthogonal multiple access (NOMA) schemes are gaining a lot of attentions for fifth generation (5G) cellular networks. As compared to the conventional orthogonal multiple access technologies, NOMA techniques can accommodate much more users via non-orthogonal resource allocation. Existing dominant NOMA schemes can be divided into two main categories: power-domain multiplexing and code-domain multiplexing. In this work, we evaluate the performance of two code-domain multiplexing techniques: interleave-division multiple access (IDMA) and non-orthogonal coded access (NOCA). We propose different detection schemes for these access schemes. Specifically, we integrate these techniques with one of the 5G air interface proposals, i.e., universal filtered multicarrier (UFMC). We compare the performance of these multiple access schemes with cyclic prefix orthogonal frequency division multiplexing (CP-OFDM) based IDMA and NOCA techniques. Our results indicate that a large number of users can be accommodated with these techniques. Moreover, using UFMC or CP-OFDM in conjunction with these code-domain multiplexing techniques provides a similar performance in a synchronous environment.**

I. Introduction

A vast number of services such as the Internet of Things (IoT) / machine-type communications (MTC) will be supported in 5G networks [1]. To fulfill these requirements, 5G networks will not only be required to provide Gbps wireless connectivity but will also provide low latency and massive machine type connectivity. This poses an important demand for suitable waveforms, multiple access techniques, and signal processing solutions. At present, orthogonal multiple access (OMA) techniques such as orthogonal frequency division multiple access (OFDMA) are used for 4G systems. The OMA schemes require a large signaling overhead and scheduling protocols to provide access and reliable transmission. In order to support ultra-high connectivity, 5G wireless systems also need to better utilize the available spectrum. One solution to fulfill these requirements is to employ non-orthogonal multiple access (NOMA) schemes in 5G for massive MTC (mMTC) [2].

The mMTC technology refers to a system where a large number of nodes in one cell transmits small-sized information packets sporadically to the base station [3]. The transmitted data could be seen as measurements collected from sensors in a large factory plant. Therefore, they need to be low-cost and low-complexity devices with long-life batteries. On the other hand, the complexity constraints at the base station could be fairly relaxed [4]. To tackle these challenges, a careful design of an appropriate NOMA scheme with multi-user detection is highly required.

NOMA techniques can be categorized into two main classes: power-domain and code-domain multiplexing [4]. In power-domain NOMA, the users are separated by different power levels, whereas the users are assigned distinctive spreading sequences in code-domain NOMA. The interleave-division multiple access (IDMA) and non-orthogonal coded access (NOCA) schemes are two popular techniques that belong to the code-domain category. In IDMA, all users share a common spreading sequence and are separated by different interleavers. On the other hand, in NOCA, non-orthogonal spreading sequences from a codebook are assigned randomly to the users. The IDMA technique was proposed in [5] and has been further investigated in [6], [7]. Especally, the performance of IDMA with universal filtered multi-carrier (UFMC) was investigated in [8]. The NOCA technique is a new multiple access scheme that was proposed in [9] and further investigated in [10]. Many aspects of this access scheme such as integration of the NOCA with CP-OFDM and other 5G waveforms, the detection procedures, and a comparison with other state of the art access schemes are still in its infancy. Therefore, in this work, we provide answers to some of these challenges. Specifically, we integrate the UFMC waveform with NOCA techniques and compare the performance of IDMA and NOCA multiple access schemes with CP-OFDM. For this purpose we propose different detection procedures.

In the following, we first review the IDMA system model and discuss the principles of NOCA (Section II). Moreover, we propose the integration of the NOCA technique with the UFMC waveform. We study and analyze sub-optimal multiuser receivers and develop an iterative receiver for NOCA in Section III. Then, we define multi-user scenarios for simulations in a link-level simulator and present the results (Section IV). The paper is summarized at the end in Section V.

Notation: Throughout this paper, scalars are represented by italic letters (a, b, A, B), vectors by lower-case bold-faced letters $(\mathbf{a}, \mathbf{b})$, and matrices are denoted as upper-case bold-faced letters $(\mathbf{A}, \mathbf{B})$. The superscripts $(\cdot)^T$ and $(\cdot)^H$ represent matrix transpose and complex conjugate transpose (Hermitian), respectively. The set of real-valued numbers is denoted by $\mathbb{R}$, and $\mathbb{C}$ represents the set of complex-valued numbers.

ISBN 978-3-8007-4541-8

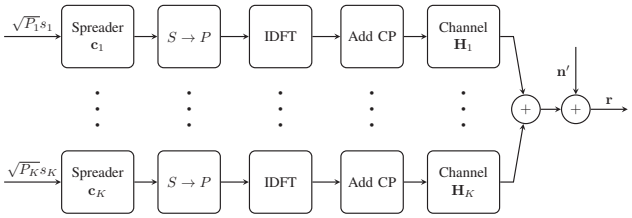

Fig. 1. NOCA transmitter using OFDM waveform

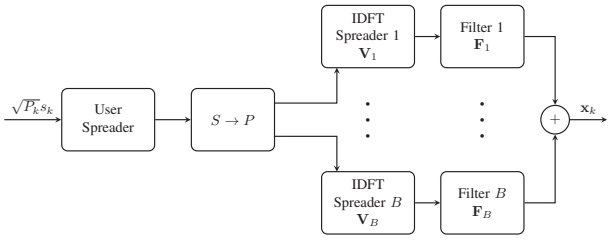

Fig. 2. NOCA transmitter using UFMC waveform

II. System Model

A. Interleave-Division Multiple Access (IDMA)

In IDMA, all users share a common spreading code for example a repetition coder, but they are separated by their unique interleavers as opposed to code-divison multiple access (CDMA). The users' information bits are encoded, spread, and interleaved. Then the resultant chip sequences are mapped into symbols and modulated onto sub-carriers by using inverse discrete Fourier Transform (IDFT) in an OFDM-IDMA system. At the receiver side, a low complexity and iterative multi-user detection (MUD) receiver is applied [11]. It consists of an elementary signal estimator (ESE) and a bank of *a posteriori* probability (APP) decoders which work in a turbo-type manner.

In an OFDM-IDMA system with K users, the received signal after the removal of the cyclic prefix and discrete Fourier transform (DFT) is given by [12]

$$\mathbf{y} = \sum_{k=1}^{K} \left(\sqrt{P_k} \mathbf{\Lambda}_k \mathbf{z}_k \right) + \mathbf{n}, \tag{1}$$

where $\mathbf{z}_k$ is the transmitted signal vector for user k, P_k the user's signal power, $\mathbf{\Lambda}_k$ a diagonal matrix with the channel frequency response on its diagonal, and $\mathbf{n}$ is additive white Gausian noise (AWGN).

B. Non-Orthogonal Coded Access (NOCA)

In the NOCA technique, Zadoff-Chu (ZC) sequences are used as spreading codes [9]. These sequences spread data symbols over multiple sub-carriers of a multi-carrier system such as CP-OFDM.

1) Zadoff–Chu Sequences: ZC sequences are widely used in LTE for the uplink reference signals [13]. A ZC sequence of length N_{ZC} is defined as

$$c_q(n) = \begin{cases} \exp(-j2\pi q \frac{n(n+1)/2+ln}{N_{ZC}}) & \text{for } N_{ZC} \text{ odd}, \\ \exp(-j2\pi q \frac{n^2/2+ln}{N_{ZC}}) & \text{for } N_{ZC} \text{ even}, \end{cases} \tag{2}$$

where $q \in \{1, 2, \ldots, N_{ZC}-1\}$ is the ZC sequence root index, $n = 0, 1, \ldots, N_{ZC}-1$ and $l \in \mathbb{N}$ is any integer. For each root sequence, N_{ZC} orthogonal sequences can be generated by cyclic shifting. However, the codes from different root indices are not orthogonal.

2) NOCA with OFDM waveform: In this section, we discuss the NOCA technique with an OFDM waveform. The block diagram of this system is shown in Fig. 1. The spreading code for each user is chosen randomly from a large codebook of ZC sequences. After users' symbols get spread, the generated chips of each user are assigned to sub-carriers of an OFDM symbol to overcome multi-path fading. The users' wireless channels, denoted by matrices $\mathbf{H}_1, \mathbf{H}_2, \cdots, \mathbf{H}_K$ in Fig. 1, are assumed unique [9].

Let us consider an uplink scenario where K users transmit data symbols $s_1, s_2, \cdots, s_K$ with signal powers $P_1, P_2, \cdots, P_K$. Theses symbols are spread in the frequency domain using spreading sequences $\mathbf{c}_1, \mathbf{c}_2, \cdots, \mathbf{c}_K$ of length S_f. The received signal vector after removing the cyclic prefix and taking DFT is given by

$$\mathbf{y} = \sum_{k=1}^{K} \left(\sqrt{P_k} \mathbf{\Lambda}_k \mathbf{c}_k s_k \right) + \mathbf{n}, \tag{3}$$

where $\mathbf{\Lambda}_1, \mathbf{\Lambda}_2, \cdots, \mathbf{\Lambda}_K$ denote the users' wireless channels in the frequency domain and $\mathbf{n}$ is AWGN.

3) NOCA with UFMC waveform: In this section, we propose the integration of the NOCA technique with the UFMC waveform. The block diagram of such a system is illustrated in Fig. 2. In UFMC, the total number of data sub-carriers are grouped in B sub-bands where a "sub-band" may represent a physical resource block in LTE terminology. We consider an uplink scenario where K users transmit data symbols $s_1, s_2, \cdots, s_K$ with signal powers $P_1, P_2, \cdots, P_K$. These symbols are spread in the frequency domain using spreading sequences $\mathbf{c}_1, \mathbf{c}_2, \cdots, \mathbf{c}_K$ of length S_f.

The generated chips of each user after the spreading are grouped in B sub-bands. Then an N-point IDFT is applied to each group. The time domain signal passes through a Dolph-Chebyshev filter with N_f coefficients. A Dolph-Chebyshev filter maximizes the side lobe attenuation for a given main lobe width [14]. The sub-band signals are added to form the transmitted signal for user k as

$$\mathbf{x}_k = \sqrt{P_k} \begin{bmatrix} \mathbf{F}_1 & \cdots & \mathbf{F}_B \end{bmatrix} \begin{bmatrix} \mathbf{V}_1 & \cdots & \mathbf{0} \\ \vdots & \ddots & \vdots \\ \mathbf{0} & \cdots & \mathbf{V}_B \end{bmatrix} \mathbf{c}_k s_k \tag{4}$$

where $\mathbf{V}_i \in \mathbb{C}^{N \times n_i}$ is the IDFT spreader matrix and $\mathbf{F}_i \in \mathbb{C}^{(N+N_f-1) \times N}$ is a Toeplitz matrix composed of the filter

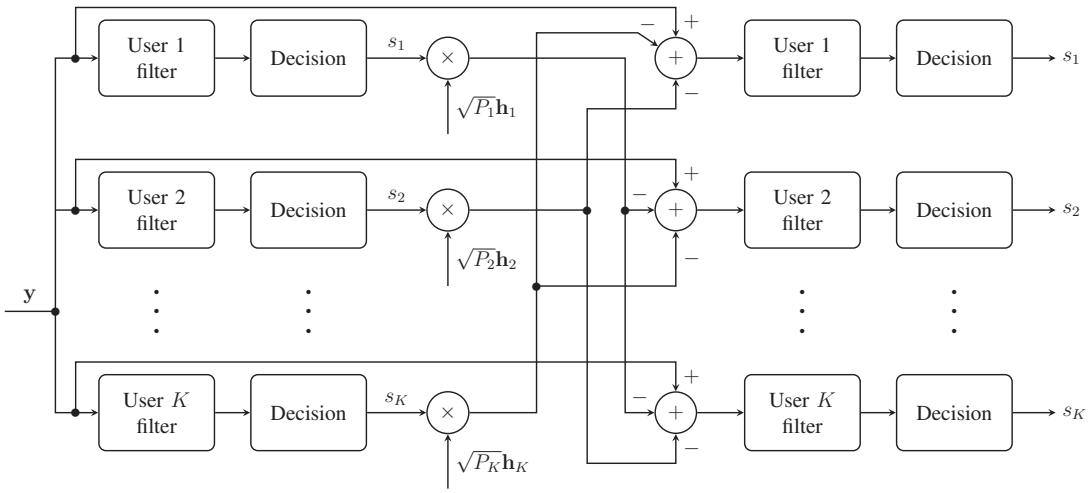

Fig. 3. Parallel interference cancellation

impulse response which executes the convolution. Note that we have chosen $n_i = 12 \quad \forall i = 1, 2, \cdots, B$.

The received signal at the base station can be written as

$$\mathbf{r} = \begin{bmatrix} \mathbf{H}_1 & \cdots & \mathbf{H}_K \end{bmatrix} \begin{bmatrix} \mathbf{FV} & \cdots & \mathbf{0} \\ \vdots & \ddots & \vdots \\ \mathbf{0} & \cdots & \mathbf{FV} \end{bmatrix} \mathbf{CPs} + \mathbf{n}' \tag{5}$$

where $\mathbf{H}_k \in \mathbb{C}^{(N+N_f-1)\times(N+N_f-1)}$ is the user's channel convolution matrix, $\mathbf{F} = \begin{bmatrix} \mathbf{F}_1 & \mathbf{F}_2 & \cdots & \mathbf{F}_B \end{bmatrix}$, $\mathbf{V}$ is a block diagonal matrix with diagonal elements $\mathbf{V}_1, \mathbf{V}_2, \cdots, \mathbf{V}_B$, $\mathbf{C} \in \mathbb{C}^{KS_f \times K}$ is also a block diagonal matrix with diagonal elements $\mathbf{c}_1, \mathbf{c}_2, \cdots, \mathbf{c}_K$, and $\mathbf{P} \in \mathbb{R}^{K\times K}$ is a diagonal matrix. Equation (5) can also be written in compact form as

$$\mathbf{r} = \sum_{k=1}^{K} \left(\sqrt{P_k} \mathbf{H}_k \mathbf{FV} \mathbf{c}_k s_k \right) + \mathbf{n}', \tag{6}$$

where $\mathbf{n}'$ is complex additive white Gaussian noise with mean zero and variance σ_n^2.

At the receiver, first the operation of overlap adding is performed, i.e., the last $N_f - 1$ samples of every received vector are added to the beginning. After taking the DFT transform, the resulting signal is given by

$$\mathbf{y} = \mathbf{DTr}, \tag{7}$$

where $\mathbf{T} \in \{0,1\}^{N\times(N+N_f-1)}$ performs the overlap adding operation and $\mathbf{D} \in \mathbb{C}^{S_f \times N}$ is the DFT matrix. Since $\mathbf{TT}^H = \mathbf{I}$ and $\mathbf{DD}^H = \mathbf{I}$, the received signal in the frequency domain can be written as

$$\mathbf{y} = \sum_{k=1}^{K} \left(\sqrt{P_k} \mathbf{\Lambda}_k \mathbf{c}_k s_k \right) + \mathbf{n}, \tag{8}$$

where $\mathbf{\Lambda}_k = \mathbf{DTH}_k\mathbf{FV}$ is a diagonal matrix containing the channel frequency response on its diagonal. Equation (8) can also be written in matrix notation as

$$\mathbf{y} = \mathbf{\Lambda CPs} + \mathbf{n}, \tag{9}$$

where $\mathbf{\Lambda} = \begin{bmatrix} \mathbf{\Lambda}_1 & \mathbf{\Lambda}_2 & \cdots & \mathbf{\Lambda}_K \end{bmatrix} \in \mathbb{C}^{S_f \times KS_f}$.

III. NOCA Multi-User Detection

In the following, we present some of the linear and non-linear estimation techniques that we employ at receivers with the NOCA technique.

A. Minimum Mean-Square Error Receiver

If the length of the spreading code is less than the number of users ($S_f < K$), the symbols are estimated by employing the following MMSE filter

$$\hat{\mathbf{s}} = \mathbf{PC}^H\mathbf{\Lambda}^H \left[\mathbf{\Lambda CP}^2\mathbf{C}^H\mathbf{\Lambda}^H + \sigma_n^2\mathbf{I} \right]^{-1} \mathbf{y}. \tag{10}$$

However, if the length of the spreading code is greater than or equal to the number of users ($S_f \geq K$), it is more efficient to apply the following filter to estimate the data symbols

$$\hat{\mathbf{s}} = \mathbf{P}^{-1} \left[\mathbf{C}^H\mathbf{\Lambda}^H\mathbf{\Lambda C} + \sigma_n^2\mathbf{P}^{-2} \right]^{-1} \mathbf{C}^H\mathbf{\Lambda}^H\mathbf{y}. \tag{11}$$

B. Parallel Interference Cancellation

The parallel interference cancellation (PIC) receivers consists of two steps as shown in Fig. 3. In the first step, an initial estimate of all signals are computed applying a filter such as MMSE. Next, the signals are reconstructed by using each user's channel frequency response and spreading sequence. These reconstructed signals, which are considered as interference to other users' signals, will be subtracted from the original received vector to better estimate the desired data at the second step. The PIC detector can be extended by cascading more stages to develop a general multi-stage receiver. In this technique, the estimations at each stage is employed to enhance the detection performance at the next stage. Based on this, we develop an iterative MMSE-PIC receiver for NOCA. This is a multi-stage detector based on the MMSE filter. The function of this receiver is summarized as follows:

1) Initial estimation of the data from all users using the linear MMSE filter,

ISBN 978-3-8007-4541-8

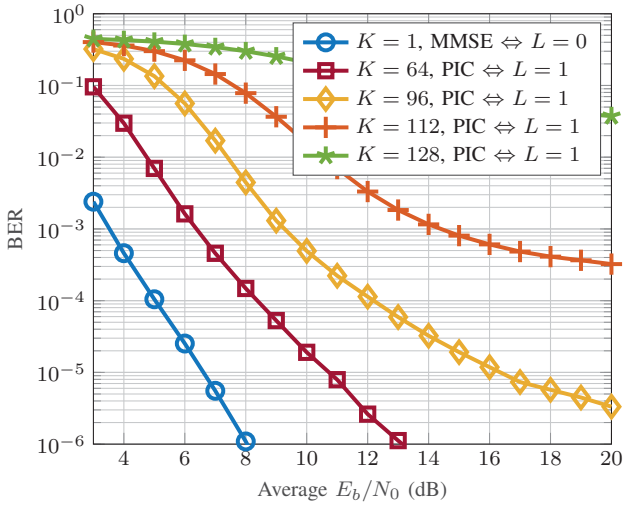

Fig. 4. Performance comparison of MMSE-PIC receiver for NOCA and different number of users, $S_f = 64$

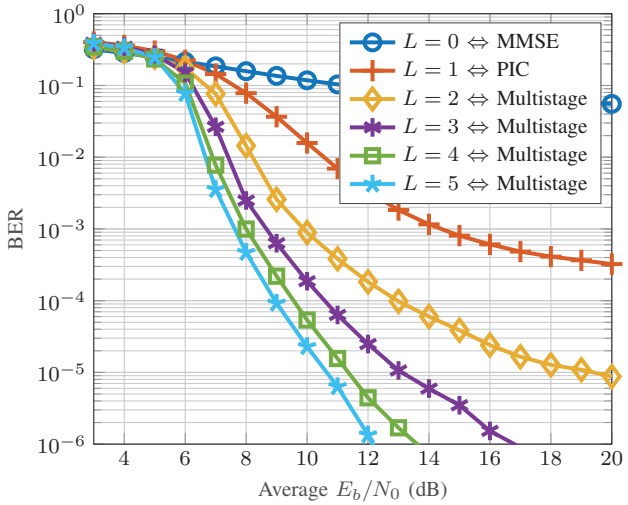

Fig. 5. NOCA Multistage receiver for $K = 112$ users and $S_f = 64$

2) Reconstructing all users' signals using their channel frequency responses and spreading sequences,
3) Subtracting the calculated interferences from the received signal for each user,
4) Re-estimation of each user's signal using the pre-calculated MMSE filter,
5) Going back to step 2 and repeating this procedure for $L - 1$ times.

IV. Simulation Results

In this section, we show some of results for the system performance of NOCA in different scenarios. We have drawn the data bits from a QPSK constellation and have also employed forward error correction codes. A convolutional encoder $(23, 35)_8$ with the coding rate of $R_c = 1/2$ is used for all users. Each packet of information contains $N = 256$ bits. A codebook of ZC sequences of length 64 is generated, and each user is randomly assigned a different sequence as a spreading code. The spreading factor is $S_f = 64$. Hence, the total coding rate is $R = R_c/S_f = 1/128$. The frame length is $J = N \times S_f = 16,384$. The results are shown for a flat Rayleigh fading channel. Moreover, we assume that the signals received from all users are synchronized and also equally powered.

The capability of the MMSE-PIC receiver to detect different numbers of NOCA users is illustrated in Fig. 4. The BER curve for a single-user is also included for reference. As shown in the figure, the MMSE-PIC is able to cope with overloading (the number of users is greater than the spreading factor). For $K = 112$, the BER of about 3×10^{-3} is achieved at $E_b/N_0 = 20$ dB. To improve its performance, we apply a MMSE multi-stage receiver whose results are demonstrated in Fig. 5. The figure shows the SNR evolution by applying more stages where we obtain the same BER at about $E_b/N_0 = 8$ dB at stage $L = 5$. That is equivalent to a gain of 12 dB.

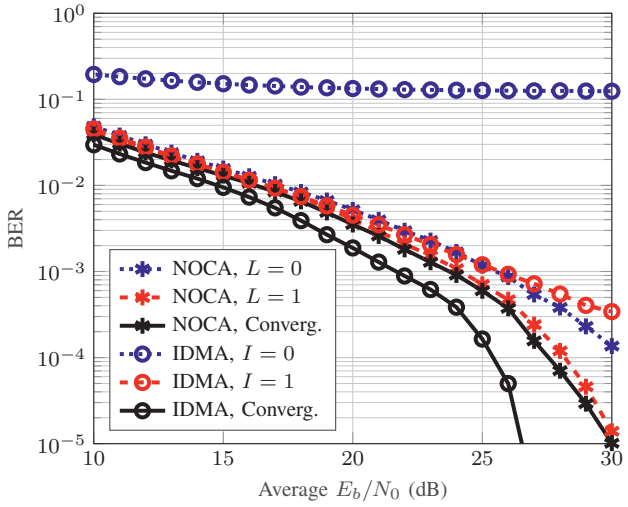

Fig. 6. Performance comparison of NOCA and IDMA with CP-OFDM waveform for $K = 60$ and $S_f = 60$

We define another scenario to compare the NOCA and IDMA techniques with the UFMC and CP-OFDM waveforms. Here, each packet of information has $N = 280$ bits and the spreading factor is $S_f = 60$. A length-60 repetition coder serves as a spreader for IDMA. The loading is 100 %, that is, all systems have $K = 60$ users. We adopt the 3GPP LTE standard to simulate the waveforms and apply the extended pedestrian A (EPA) channel [15]. We apply exactly the same channel impulse response (CIR) for all systems. Perfect knowledge of CIR is assumed at the receiver, and channel equalization is carried out in the frequency domain. The number of DFT points is $N_{\text{FFT}} = 128$ as well as the number of total sub-carriers.

The performance of the NOCA technique with the OFDM waveform is compared with IDMA in Fig. 6. It shows the convergence behavior of both schemes where I indicates

ISBN 978-3-8007-4541-8

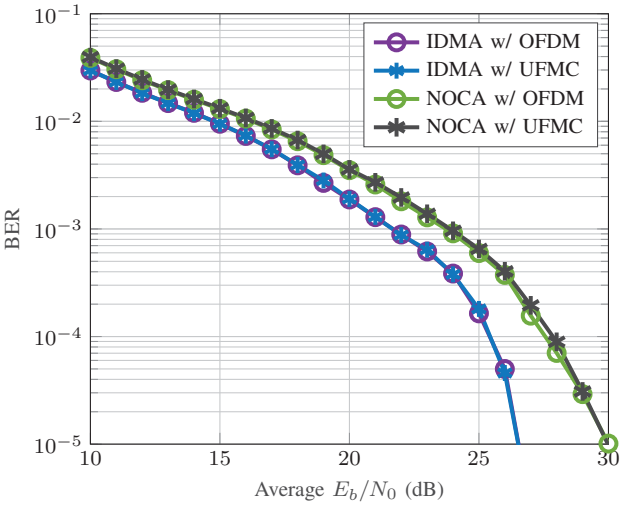

Fig. 7. Performance comparison of NOCA and IDMA with UFMC and CP-OFDM waveforms for $K = 60$ and $S_f = 60$

the number of iterations for the IDMA multiuser detector. Moreover, we add the UFMC waveform in Fig. 7. The results indicate that both waveforms perform equally well in a synchronous environment. However, the UFMC waveform has better spectral properties and is expected to perform much better in an asynchronous environment. Fig. 7 also shows the comparison of NOCA with IDMA. It is observed that the IDMA technique outperforms the NOCA scheme for the converged performance. The achieved gain in case of IDMA is about 3.5 dB at a BER of 10^{-5} in contrast to the NOCA system.

V. Conclusion

In this paper, we conducted a detailed study of the principles and key features of NOCA as a non-orthogonal multiple access technique proposed for 5G. Moreover, the NOCA scheme was integrated with the UFMC waveform and compared to IDMA with respect to the BER performance. We also investigated different estimation techniques for NOCA and developed an iterative MMSE-PIC receiver for this scheme. The NOCA capability of supporting a large number of users in order to support mMTC in 5G were also analyzed in this work. The systems were simulated by adopting the current 3GPP LTE standards and its channel model (EPA) in a link-level simulator.

Acknowledgment

This work has been performed in the framework of the Horizon 2020 project ONE5G (ICT-760809) receiving funds from the European Union. The authors would like to acknowledge the contributions of their colleagues in the project, although the views expressed in this contribution are those of the authors and do not necessarily represent the project.

References

[1] G. Wunder, P. Jung, M. Kasparick, T. Wild, F. Schaich, Y. Chen, S. T. Brink, I. Gaspar, N. Michailow, A. Festag, L. Mendes, N. Cassiau, D. Ktenas, M. Dryjanski, S. Pietrzyk, B. Eged, P. Vago, and F. Wiedmann, "5GNOW: non-orthogonal, asynchronous waveforms for future mobile applications," *IEEE Communications Magazine*, vol. 52, no. 2, pp. 97–105, February 2014.

[2] Z. Ding, Y. Liu, J. Choi, Q. Sun, M. Elkashlan, C. L. I, and H. V. Poor, "Application of non-orthogonal multiple access in LTE and 5G networks," *IEEE Communications Magazine*, vol. 55, no. 2, pp. 185–191, February 2017.

[3] C. Bockelmann, N. Pratas, H. Nikopour, K. Au, T. Svensson, C. Stefanovic, P. Popovski, and A. Dekorsy, "Massive machine-type communications in 5G: physical and MAC-layer solutions," *IEEE Communications Magazine*, vol. 54, no. 9, pp. 59–65, September 2016.

[4] L. Dai, B. Wang, Y. Yuan, S. Han, C. l. I, and Z. Wang, "Non-orthogonal multiple access for 5G: solutions, challenges, opportunities, and future research trends," *IEEE Communications Magazine*, vol. 53, no. 9, pp. 74–81, September 2015.

[5] L. Ping, L. Liu, K. Y. Wu, and L. WK, "On interleave-division multiple-access," in *2004 IEEE International Conference on Communications*, vol. 5, June 2004, pp. 2869–2873 Vol.5.

[6] L. Ping, Q. Guo, and J. Tong, "The OFDM-IDMA approach to wireless communication systems," *IEEE Wireless Communications*, vol. 14, no. 3, pp. 18–24, June 2007.

[7] Z. Li, L. Li, Z. Wu, and W. Wang, "Uplink transmission technique for interleave-division multiple-access on block fading channel," in *2010 2nd IEEE International Conference on Network Infrastructure and Digital Content*, Sept 2010, pp. 546–550.

[8] Y. Chen, F. Schaich, and T. Wild, "Multiple access and waveforms for 5G: IDMA and universal filtered multi-carrier," in *IEEE 79th Vehicular Technology Conference (VTC Spring)*, May 2014, pp. 1–5.

[9] Z. Zhao, D. Miao, Y. Zhang, J. Sun, H. Li, and K. Pedersen, "Uplink contention based transmission with non-orthogonal spreading," in *2016 IEEE 84th Vehicular Technology Conference (VTC-Fall)*, Sept 2016, pp. 1–6.

[10] Q. Wang, Z. Zhao, D. Miao, Y. Zhang, J. Sun, and Z. Zhong, "Non-orthogonal coded access for contention-based transmission in 5G," in *Proc. of Veh. Technol. Conf. Fall (VTC17 Fall)*, Sept 2017.

[11] L. Ping, L. Liu, K. Wu, and W. K. Leung, "Interleave-division multiple-access," *IEEE Transactions on Wireless Communications*, vol. 5, no. 4, pp. 938–947, April 2006.

[12] Q. Guo, X. Yuan, and L. Ping, "Single- and multi- carrier idma schemes with cyclic prefixing and zero padding techniques," *European Transactions on Telecommunications*, vol. 19, no. 5, pp. 537–547, 2008. [Online]. Available: http://dx.doi.org/10.1002/ett.1266

[13] S. Sesia, I. Toufik, and M. Baker, *LTE - The UMTS Long Term Evolution: From Theory to Practice*, 2nd ed. John Wiley & Sons, 2011.

[14] T. Wild, F. Schaich, and Y. Chen, "5G air interface design based on universal filtered (UF-)OFDM," in *Digital Signal Processing (DSP), 2014 19th International Conference on*, Aug 2014, pp. 699–704.

[15] 3GPP, "Evolved Universal Terrestrial Radio Access (E-UTRA); Base Station (BS) radio transmission and reception," 3rd Generation Partnership Project (3GPP), TS 36.104, Jul 2015. [Online]. Available: http://www.3gpp.org/ftp/Specs/archive/36_series/36.104/36104-c80.zip

